Plant Physiology Preview. Published on January 15, 2013, as DOI:10.1104/pp.112.211029

Running head: An antagonistic peptide technology

Corresponding author: Chun-Ming Liu

Institute and Address:
Key Laboratory of Plant Molecular Physiology, Institute of Botany, Chinese Academy of Sciences, Nanxincun 20, Fragrant Hill, Beijing 100093, China

Email: cmliu@ibcas.ac.cn

Tel and Fax: 0086-10-6283-6663

The author responsible for distribution of materials integral to the findings presented in this article in accordance with the policy described in the Instructions for Authors (www.plantphysiol.org) is: Chun-Ming Liu (cmliu@ibcas.ac.cn).

Number of words used	6,667
Figures:	8
Supplemental Figures:	4
Supplemental Tables:	1

Copyright 2013 by the American Society of Plant Biologists

Antagonistic Peptide Technology for Functional Dissection of *CLE* Genes in Arabidopsis

Xiu-Fen Song,[1] Peng Guo,[1,2] Shi-Chao Ren,[1,2] Ting-Ting Xu,[1,2] Chun-Ming Liu[1]*

[1]Key Laboratory of Plant Molecular Physiology, Institute of Botany, Chinese Academy of Sciences, Nanxincun 20, Fragrant Hill, Beijing 100093, China
[2]Graduate University of Chinese Academy of Sciences, Beijing 100049, China

***Corresponding author**
Email: cmliu@ibcas.ac.cn
Tel and Fax: 0086-10-6283-6663

FOOTNOTES

This work was supported by the Ministry of Science and Technology of China (SQ2012CC057223), the National Natural Science Foundation of China (31121065), and the Chinese Academy of Sciences (200904910192008).

ABSTRACT

In recent years, peptide hormones have been recognized as important signal molecules in plants. Genetic characterization of such peptides is challenging since they are usually encoded by small genes. As a proof of concept, we used the well-characterized stem cell-restricting CLV3 to develop an antagonistic peptide technology by transformations of wildtype Arabidopsis with constructs carrying the full-length *CLV3* with every residues in the peptide-coding region replaced, one at a time, by Ala. Analyses of transgenic plants allowed us to identify one line exhibited a dominant-negative *clv3*-like phenotype, with enlarged shoot apical meristems and increased numbers of floral organs. We then performed second dimensional amino acid substitutions to replace the Gly residue individually with the other 18 possible proteinacious amino acids. Examination of transgenic plants showed that a Gly to Thr substitution gave the strongest antagonistic effect in the wildtype, in which over 70% of transgenic lines showed the *clv3*-like phenotype. Among these substitutions, a negative correlation was observed between the antagonistic effects in the wildtype and the complementation efficiencies in *clv3*. We also demonstrated that such an antagonistic peptide technology is applicable to other *CLV3/ESR* (*CLE*) genes, *CLE8* and *CLE22,* as well as *in vitro* treatments. We believe this technology provides a powerful tool for functional dissection of widely occurring *CLE* genes in plants.

INTRODUCTION

In animals, small peptides are important signal molecules in neural and endocrinal systems (Edlund and Jessell, 1999). In recent years, over a dozen different types of peptide hormones have been identified in plants, regulating both developmental and adaptive responses, usually through interacting with leucine-rich repeat receptor kinases (LRR-RK) localized in plasma membranes of neighboring cells (Boller and Felix, 2009; De Smet et al., 2009; Katsir et al., 2011). These peptides are often produced from genes with small open reading frames (ORFs), after post-translational processing (Matsubayashi, 2011). In addition, peptide hormones such as CLV3/ESR (CLE), systemin, PSK, AtPEP1 and EPF1 often have paralogues in genomes (Cock et al., 2001; Pearce et al., 2003; Yang et al., 2001; Huffaker et al., 2006; Hara et al., 2009). Bioinformatics analyses revealed that the Arabidopsis genome contains 33,809 small ORFs (Lease et al., 2006).

CLV3 acts as a secreted 12- or 13-amino acid (AA) glycosylated peptide (Kondo et al., 2006; Ohyama et al., 2009) to restrict the number of stem cells in shoot apical meristems (SAM), through a CLV1-CLV2-SOL2 (also called CRN)-RPK2 receptor kinase-mediated pathway (Clark et al., 1993; Jeong et al., 1999; Miwa et al., 2008; Müller et al., 2008; Kinoshita et al., 2010; Zhu et al., 2010). All CLV3/ESR (CLE) family members, of which there are 83 in Arabidopsis and 89 in rice, carry a putative signal peptide and share a conserved 12 AA core CLE motif (Oelkers et al. 2008). Over-expression of *CLE* genes often shows a common dwarf and short-root phenotype (Strabala et al., 2006; Jun et al., 2010), which may not reflect their endogenous functions. Due to redundancies and difficulties in identifying mutants of these small genes, studies of CLE members are challenging. Only a few *CLE* genes have been genetically characterized, in particular, *CLV3*, *CLE8*, *CLE40* and *CLE41* in Arabidopsis and *FON4*, *FCP1* and *FOS1* in rice (Fletcher et al., 1999; Fiume and Fletcher, 2012; Hobe et al., 2003; Etchells and Turner, 2010; Chu et al., 2006; Suzaki et al., 2008; Suzaki et al., 2009), while functions of other CLE members remain unknown.

As a proof of concept, we used the well-characterized *CLV3* gene to develop an antagonistic peptide technology for functionally dissecting CLE

family members in Arabidopsis. A series of constructs carrying Ala substitutions in every AA residue in the core CLE motif of CLV3, expressed under the endogenous *CLV3* regulatory elements, were made and introduced to wildtype Arabidopsis by transformation. This allowed us to identify the conserved Gly residue in the middle of the CLE motif was vulnerable for generating the dominant-negative *clv3*-like phenotype. We then performed second dimensional AA substitutions to replace the Gly with all other 18 possible proteinacious AA, one at a time, and observed that the substitution of the Gly residue by Thr generated the strongest dominant-negative *clv3*-like phenotype. Further experiments showed that this technology can potentially be applied to *in vitro* synthesized peptides and for functional characterization of other CLE members.

RESULTS AND DISCUSSION

Transgenic Plants Carrying CLV3 with the Gly to Ala Substitution in the Core CLE Motif Showed a Dominant-Negative *clv3*-like Phenotype

The full-length 3,932 bp *CLV3* genomic sequence including a 1,857 bp 5'-upstream sequence, a 559 bp coding region, and a 1,516 bp 3'-downstream sequence was amplified (named *CLV3F*) and cloned as previously described (Song et al., 2012). Using *CLV3F* as the template, 12 constructs (named $CLV3_{Ala1\text{-}12}$) were made via PCR-based site-directed mutagenesis to replace each of the 12 residues with Ala, one at a time, in the core CLE motif of CLV3 (Fig. 1A; Song et al., 2012), and transformed into wildtype Arabidopsis (ecotype L*er*) to obtain at least 30 independent transgenic plants for each construct. We screened these transgenic plants for the multi-carpel *clv3* mutant-like phenotype. As controls, wildtype and transgenic plants carrying *CLV3F* consistently showed two-carpel siliques (Fig. 1B). Although most plants carrying $CLV3_{Ala1\text{-}12}$ showed no phenotype, we identified that one plant carrying $CLV3_{Ala6}$, with the Gly residue at the position 6 substituted by Ala, exhibited multiple carpels (3 to 4 carpels) in siliques (Fig. 1, B-D), resembling a weak *clv3* phenotype. Sequencing of the endogenous *CLV3* locus from the transgenic plant revealed no mutations, suggesting that the observed phenotype is not likely due to contamination from a recessive *clv3* mutant.

The $CLV3_{Ala6}$ transgenic line was backcrossed to the wildtype, and BC1 plants still exhibited the *clv3*-like phenotype (Fig. 1, E and F), suggesting a dominant trait. Phenotypic analyses in the T2 generation showed that the phenotype can be stably transmitted. Transgenic plants carrying the remaining 11 constructs did not give the *clv3*-like phenotype (Fig. 1B), suggesting that the Gly residue in the CLE motif is vulnerable in creating the antagonistic effect. It is plausible that peptides produced by the $CLV3_{Ala6}$ transgene are able to compete with the endogenous CLV3 peptides antagonistically to bind the CLV1-CLV2-SOL2-RPK2 receptor kinases and then block downstream signal transduction.

Optimization of the Antagonistic Peptide Technology through Second Dimensional AA Substitutions

Since the Gly to Ala substitution in CLV3 generated only a mild antagonistic effect in the wildtype (Fig. 1B), we performed second dimensional AA substitutions by replacing the Gly residue, one at a time, with all other 18 possible proteinacious AAs through site-directed mutagenesis (Fig. 1A). All constructs, *CLV3*$_{Leu6}$, *CLV3*$_{Ile6}$, *CLV3*$_{Val6}$, *CLV3*$_{Phe6}$, *CLV3*$_{Trp6}$, *CLV3*$_{Pro6}$, *CLV3*$_{Met6}$, *CLV3*$_{Cys6}$, *CLV3*$_{Ser6}$, *CLV3*$_{Thr6}$, *CLV3*$_{Tyr6}$, *CLV3*$_{Asn6}$, *CLV3*$_{Gln6}$, *CLV3*$_{Lys6}$, *CLV3*$_{Arg6}$, *CLV3*$_{His6}$, *CLV3*$_{Asp6}$ and *CLV3*$_{Glu6}$ were transformed into wildtype Arabidopsis (L*er*), and at least 30 independent transformants were obtained for each construct. For each T1 transgenic plant, 15 siliques (5 from the bottom, 5 from the middle and 5 from the top of the inflorescence) were excised and examined under a dissection microscope for carpel numbers. Efficiencies of these constructs in creating the dominant-negative *clv3*-like phenotype are summarized in Fig. 2A, based on examination of over 700 independent transgenic lines. Strikingly, all these constructs, excluding *CLV3*$_{Tyr6}$, were able to produce some plants with the *clv3*-like phenotype (Fig. 2A). Plants carrying *CLV3*$_{Thr6}$ showed the highest antagonistic effect, with approximately 70% of the *CLV3*$_{Thr6}$ transgenic lines exhibiting the multi-carpel phenotype (Figs. 2A and 3A). Constructs of *CLV3*$_{Phe6}$, *CLV3*$_{Leu6}$, *CLV3*$_{Pro6}$, *CLV3*$_{Ile6}$, *CLV3*$_{Gln6}$, *CLV3*$_{Lys6}$, *CLV3*$_{Trp6}$, *CLV3*$_{Val6}$ and *CLV3*$_{Asn6}$ gave a moderate antagonistic effect, in which 35-60% of lines showed the *clv3*-like phenotype (Fig. 2A). The other 7 constructs including *CLV3*$_{Ser6}$, *CLV3*$_{Met6}$, *CLV3*$_{Arg6}$, *CLV3*$_{Cys6}$, *CLV3*$_{His6}$, *CLV3*$_{Asp6}$ and *CLV3*$_{Glu6}$ gave only a weak antagonistic effect (Fig. 2A). Transformation of *CLV3*$_{Tyr6}$ led to no antagonistic effect, all 102 *CLV3*$_{Tyr6}$ transgenic lines examined resembled wildtype plants. Results from phenotypic analyses in 43 individual transgenic plants carrying *CLV3*$_{Thr6}$ are shown in Fig. 3A. The carpel numbers per silique varied from 2 to 7 among different transgenic lines (Fig. 3, A and B). No two-carpel siliques were observed in some lines, such as No. 8, 11, 21 and 38, suggesting that there was a very strong antagonistic effect (Fig. 3A). Further analyses revealed increased numbers of flower buds in inflorescences (Fig. 3C), and enlarged SAMs in seedlings (Fig. 3D), which resemble the *clv3* phenotype (Fig. 3, C and D). By comparison to constructs which gave high percentages of plants with the *clv3*-like phenotype, we noticed that substitutions of the Gly residue with other non-polar AAs carrying a longer side chain, such as Leu, Ile,

Val, Phe, Try and Pro were more likely to generate the antagonistic effect (Fig. 2A). Interaction analyses between these antagonistic peptides and CLV1, CLV2, SOL2 and RPK2 receptor proteins may help to further understand the observed antagonistic effect.

To elucidate if the *CLV3*$_{Thr6}$ transgene indeed interferes with stem cell maintenance in SAMs, we crossed the *CLV3*$_{Thr6}$ transgenic plant with the stem cell reporter line *pCLV3::GUS* (Lenhard et al., 2002), and examined the *GUS* expression in the F2 generation. We observed a prolonged *CLV3* expression in floral buds (Fig. 4A), and an enlarged *CLV3* expression domain in SAMs (Fig. 4B), as in *clv3-2* (Fig. 4), indicating that stem cell maintenance in these *CLV3*$_{Thr6}$ transgenic plants was indeed disturbed. This result confirmed that the phenotype produced by the *CLV3*$_{Thr6}$ transgene in wildtype background is similar to the phenotype of *clv3*.

To exclude the possibility that the *clv3*-like phenotype of *CLV3*$_{Thr6}$ transgenic plants resulted from co-suppression of *CLV3*, we examined the expression of endogenous *CLV3* in *CLV3*$_{Thr6}$ transgenic plants with real-time quantitative PCR. Shoot apices were dissected from seedlings of wildtype (L*er*) and *CLV3*$_{Thr6}$ transgenic plants in parallel for RNA extraction. Real-time quantitative PCRs was performed using the same forward primer and two reverse primers in which two 3' terminal nucleotides were unique, in order to discriminate between the endogenous *CLV3* and the *CLV3*$_{Thr6}$ transgene. No significant reduction of endogenous *CLV3* expression was observed in *CLV3*$_{Thr6}$ transgenic plants when compared with that in L*er* wildtype (p=0.182; Supplemental Fig. S1), suggesting that there is no co-suppression occurring. To be noted, the expression level of the *CLV3*$_{Thr6}$ transgene was higher than that of endogenous *CLV3* in the transgenic line (Supplemental Fig. S1).

Complementation Efficiencies of Second Dimensional Substitution Constructs in *clv3-2*

To characterize the relationship between antagonistic effects in the wildtype and complementation efficiencies in *clv3-2*, we transformed the second dimensional substitution constructs described above into *clv3-2* mutants and analyzed their complementation efficiencies. The results showed that approximately 20-30% of T1 transgenic plants carrying *CLV3*$_{Ser6}$

or*CLV3*$_{Cys6}$ (Fig. 2B), and 10-20% of lines carrying *CLV3*$_{His6}$, *CLV3*$_{Asp6}$ or *CLV3*$_{Glu6}$ exhibited complete complementation, producing plants with two-carpel siliques (Fig. 2B). Less than 10% of transgenic lines carrying *CLV3*$_{Gln6}$, *CLV3*$_{Asn6}$ or *CLV3*$_{his6}$ showed complete complementation (Fig. 2B). No complementation was observed in transgenic *clv3-2* plants carrying *CLV3*$_{Leu6}$, *CLV3*$_{Ile6}$, *CLV3*$_{Val6}$, *CLV3*$_{Phe6}$, *CLV3*$_{Trp6}$, *CLV3*$_{Pro6}$, *CLV3*$_{Met6}$, *CLV3*$_{Thr6}$, *CLV3*$_{Try6}$ or *CLV3*$_{Arg6}$ (Fig. 2B), suggesting that these substitutions disrupted the function of *CLV3* completely.

A somewhat negative correlation was observed between the efficiencies of the antagonistic effect in the wildtype (Fig. 2A) and the complementation effect in *clv3-2* (Fig. 2B) in the second dimensional substitution constructs. In particular, the *CLV3*$_{Thr6}$ construct produced the strongest antagonistic effect in the wildtype, but showed no complementation in *clv3-2* (Fig. 2, A and B), whereas *CLV3*$_{Glu6}$ showed the weakest antagonistic effect in the wildtype but a relatively high complementation efficiency in *clv3-2* (Fig. 2, A and B). This negative correlation would be expected if peptides produced by constructs with dominant-negative effect bind more strongly with the CLV3 receptors than the endogenous one, but fail to execute signal transduction, thereby producing the observed antagonistic effect. For the same reason, such a construct should have a reduced complementation capacity in *clv3-2*. The *CLV3*$_{Tyr6}$ construct was an exception to this observed trend, as neither an antagonistic nor a complementation effect was observed (Fig. 2, A and B). It is possible that the CLV3$_{Tyr6}$ peptide produced with the Gly to Tyr substitution lost both of the activities of interacting with CLV3 receptors, and executing downstream signal transduction.

The reason that the substitutions of the Gly residue with other AAs gave rise to the antagonistic effect in the wildtype remains to be elucidated. Studies in mouse have shown that substitution of the most critical residue in the immunogenic Hb(64-76) peptide resulted in a complete loss of downstream responses in T-cells, while substitutions of two secondarily important residues created antagonistic effects (Evavold et al., 1993). Our previous *in vivo* complementation experiments for Ala-substituted CLV3 (Song et al., 2012) have ranked this Gly residue as the third most important one for complementing *clv3-2* among the 12 residues in the core CLE motif.

Substitution of the Gly with other non-polar AAs with a longer side chain would restrict the rotation of the peptide produced, which may in turn lead to stronger receptor binding. It is plausible that the Gly to Thr substitution in CLV3 led to a non-functional yet strong receptor-binding peptide, preventing downstream signal transduction, and thereby generating the antagonistic effect.

The Antagonistic Effect *in vitro*

It has been reported previously that synthetic 12- to 14-AA peptides corresponding to the CLE motif of CLV3 are functional *in vitro* in complementing *clv3-2* (Fiers et al., 2005; Kondo et al., 2006; Ohyama et al., 2009). To investigate if the antagonistic effect also occurs *in vitro*, synthetic 12-AA CLV3 peptides with the same Gly residue replaced by Thr (named $CLV3p12_{Thr6}$) were applied to L*er* wildtype seedlings in a liquid culture at a concentration of 10 µM, as previously described (Song et al., 2012). To prevent the potential degradation of the applied peptides, media with fresh peptides was replaced every day during the 9-d treatment. Under a differential interference contrast (DIC) microscope, enlarged SAMs were observed in $CLV3p12_{Thr6}$-treated seedlings, while no enlargements were observed in the control samples incubated in media without peptide (Fig. 5, A and B). A slight reduction of SAM size was observed in seedlings treated with normal CLV3 peptides (named CLV3p12), as reported previously (Kinoshita et al., 2007; Fig. 5, A and B).This result confirmed the presence of the antagonistic effect of the $CLV3p12_{Thr6}$ peptide *in vitro*. We noticed that the sizes of SAMs in $CLV3p12_{Thr6}$-treated seedlings were much smaller than those in transgenic plants carrying $CLV3_{Thr6}$ (Figs. 3D and 5B), which suggests that the peptides applied *in vitro* were less effective than the peptides produced *in vivo* by the transgene.

To clarify if the antagonistic effect resulted from competition between $CLV3p12_{Thr6}$ and CLV3p12, we applied CLV3p12 in combination with 1, 2, and 10 times the amount of $CLV3p12_{Thr6}$ to L*er* wildtype seedlings. Media with fresh peptides was replaced every day, as described above. After a 9-d treatment, shoot apices were dissected and sizes of SAMs were measured under a DIC microscope. The meristem size of 500 um^2 was used to assign meristems with a significant reduction after peptide treatments. About 17% of

meristems treated with CLV3p12 were above 500 μm^2 in size. Under the treatments with mixed CLV3p12 and $CLV3p12_{Thr6}$, significantly increased numbers of SAMs were larger than 500 μm^2 (Supplemental Fig. S2). As the concentration of $CLV3p12_{Thr6}$ increased, the percentage of lines with SAMs larger than 500 μm^2 increased accordingly (Supplemental Fig. S2). These results suggested that $CLV3p12_{Thr6}$ can compete with CLV3p12 *in vitro* (Supplemental Fig. S2). It is noteworthy that even when ten times more $CLV3p12_{Thr6}$ was added to the medium, a complete loss of CLV3p12 activity was still not observed. Since the endogenous mature CLV3 peptide has both hydroxylation and glycosylation modifications that contribute to the CLV3 activity (Ohyama et al., 2009; Shinohara et al., 2012), the competition observed *in vitro* may not entirely represent the *in vivo* status.

Application of the Antagonistic Peptide Technology to *CLE8*

It was reported recently that mutation or down-regulation of *CLE8* in Arabidopsis leads to defective embryo and endosperm development (Fiume and Fletcher, 2012). We used *CLE8* as an additional target to examine if the antagonistic peptide technology can be used for functional dissection of other *CLE* genes in Arabidopsis. A $CLE8_{Thr6}$ construct was made, with the Gly residue at the position 6 replaced by Thr, and expressed under the native *CLE8* regulatory elements including both the 5'-upstream (1,881 bp) and 3'-downstream (1,455 bp) genomic regions. We used the same Arabidopsis Col-0 ecotype as in the *cle8-1* study reported before (Fiume and Fletcher, 2012) to perform this experiment, in order to avoid potential interference from the genetic background.

Among 78 independent $CLE8_{Thr6}$ T1 transgenic lines examined, 8 showed embryo-lethal phenotypes (Fig. 6, A and B). The percentages of embryo-lethal seeds in these transgenic lines varied from 6% to 30% (n>200 each). Phenotypes of defective embryos were similar to those reported in *cle8-1* mutants and *CLE8* down-regulated plants (Fiume and Fletcher, 2012), with abnormal cell division in the suspensor and the lower portion of the embryo at the pro-globular stage (Fig. 6, C-F). When wildtype embryos reached the cotyledonary stage (Fig. 6G), some embryos in $CLE8_{Thr6}$ transgenic lines were arrested, with altered cell division patterns (Fig. 6, H and I). The embryo defect

phenotype was also observed in the BC1 generation when the transgenic plants were pollinated reciprocally with the wildtype, suggesting a dominant trait. This result suggested that the Gly to Thr substitution in CLE8 is able to mimic the *cle8-1* mutant phenotype, indicating that the antagonistic peptide technology can be applied to elucidate additional *CLE* genes.

Application of the Antagonistic Peptide Technology to *CLE22*

To further verify the applicability of the technology, *CLE22* with unknown function was chosen as another target for the Gly to Thr substitution. A previous report has shown that *CLE22* is expressed in differentiating vascular bundles (Jun et al., 2010). The $CLE22_{Thr6}$ construct was made and transformed into the Col-0 wildtype background and expressed under the *CLE22* native promoter including 1,495 bp 5'-upstream and 1,243 bp 3'-downstream sequences. In the T2 generation, we observed that some transgenic seedlings exhibited a very short root phenotype (Fig. 7, A and B). Detailed examination revealed an almost immediate termination of the root meristem (Fig. 7, C and D). We speculated that the short-root phenotype is the consequence of arrested cell division and differentiation in roots. After crossing the $CLE22_{Thr6}$ transgenic plant with a *DR5::GUS* marker line (Ulmasov et al., 1997), we observed no *GUS* expression in the defective primary root meristem, suggesting the auxin maximum has disappeared. It remains to be elucidated whether the $CLE22_{Thr6}$ antagonistic effect interferes directly with the auxin flow in roots, or whether it interferes with vascular differentiation first and consequently disrupts auxin flow (Fig. 7, E and F).

Among all proteinacious AAs, Gly is the most flexible one, which may give peptides a free rotation property. The Gly to Thr substitutions in the core CLE motif of CLV3, CLE8 and CLE22 may have compromised the flexibility of the peptides produced, leading to stronger interaction with corresponding receptors but disrupted downstream signal transduction, therefore creating the observed antagonistic effects (Fig. 8). Sequence alignment showed that the Gly residue located in the middle of the core CLE motif is highly conserved in the CLE family, with 90.4% identity among the 198 CLE members examined (Supplemental Fig. S3). The conserved Gly residue has also been found in several other types of peptide hormones, such as AtPEPs and EPFs in plants

(Supplemental Fig. S4). Targeted expression of these genes with the Gly to Thr substitution may potentially help to characterize their functions.

CONCLUSION

Taken together, through two-dimensional AA substitutions of CLV3 and expressed under its endogenous promoters in the wildtype, we identified the Gly in the peptide-coding region as the vulnerable residue in creating the antagonistic effect. Among all proteinacious AAs tested, substitution of the Gly residue by Thr in CLV3 gave the strongest dominant *clv3* mutant-like phenotype. We further showed that the antagonistic peptide technology is effective in generating dominant-negative phenotype in CLE8 and CLE22. We believe that the technology provides a powerful tool for the functional dissection of CLEs in plants, and may potentially be used in the study of other peptide hormones.

MATERIALS AND METHODS

Plant Materials and Growth Conditions

Wildtype *Arabidopsis thaliana,* ecotype Landsberg *erecta* (L*er*), was used for all experiments except as otherwise noted. Seeds of L*er* and *clv3-2* (in L*er* background) were surface-sterilized for 2 h in a desiccator with chlorine gas as previously reported (Fiers et al., 2005), and plated on 1/2 Murashige and Skoog's basal salt medium containing 1% sucrose, 0.05% 2-(N-morpholino) ethane sulfonic acid (MES) and 1% agar (pH 5.8). After a 2-d vernalization at 4°C, plates were cultured in a growth room with 16 h light per day at 21±1°C. After a 5-d culture, seedlings were transferred to pots filled with 1:1 mixed soil and vermiculite, and grown under the same temperature and light regime. Transformation was performed via an *Agrobacterium tumefaciens*-mediated floral dip method (Clough and Bent, 1998). Transgenic plants were obtained under the selection of 25 mg/L glufosinate ammonium (Sigma, Shanghai).

Molecular Cloning

A *CLV3* genomic sequence (3,932 bp) containing 5'- and 3'-regulatory elements was cloned into a *pDONR221* vector (Life Technologies, Shanghai), and then sub-cloned into a *pBGWFS7* binary vector (Karimi et al., 2002) to produce the *CLV3F* construct. Ala-substituted *CLV3* constructs, $CLV3_{Ala1}$, $CLV3_{Ala2}$, $CLV3_{Ala3}$, $CLV3_{Ala4}$, $CLV3_{Ala5}$, $CLV3_{Ala6}$, $CLV3_{Ala7}$, $CLV3_{Ala8}$, $CLV3_{Ala9}$, $CLV3_{Ala10}$, $CLV3_{Ala11}$ and $CLV3_{Ala12}$, were made as described previously (Song et al., 2012). For the second dimensional substitutions, the Gly residue at position 6 of the core CLE motif of CLV3 was replaced by all 18 possible proteinacious AAs, one at a time, with a PCR-based site-directed mutagenesis kit (Transgen, Beijing) to produce the constructs: $CLV3_{Leu6}$, $CLV3_{Ile6}$, $CLV3_{Val6}$, $CLV3_{Phe6}$, $CLV3_{Trp6}$, $CLV3_{Pro6}$, $CLV3_{Met6}$, $CLV3_{Cys6}$, $CLV3_{Ser6}$, $CLV3_{Thr6}$, $CLV3_{Tyr6}$, $CLV3_{Asn6}$, $CLV3_{Gln6}$, $CLV3_{Lys6}$, $CLV3_{Arg6}$, $CLV3_{His6}$, $CLV3_{Asp6}$and $CLV3_{Glu6}$. A full-length 3,597 bp *CLE8* and a 3,050 bp *CLE22* genomic sequence containing 5'- and 3'- regulatory elements were cloned into the *pDONR221* vector to produce the *pDONR221-CLE8F* and *pDONR221-CLE22F*, respectively. A Gly to Thr substitution was introduced to

the CLE motif of CLE8 and CLE22 via a site-directed mutagenesis to produce the *CLE8*$_{Thr6}$ and *CLE22*$_{Thr6}$ construct.

Tissue Clearing

Samples of shoot apices, ovules and roots were cleared as described (Sabatini et al., 1999), and observed under a DIC microscope (Leica DM4500, Germany). SAM areas were measured with ImageJ software as reported previously (Fiers et al., 2005).

***In vitro* Peptide Assay**

CLV3p12 (RTVPSGPDPLHH) and CLV3p12$_{Thr6}$ (RTVPSTPDPLHH) peptides (≥90% purity) were synthesized commercially (AuGCT Biotechnology, Beijing). *In vitro* treatments of L*er* wildtype seedlings with 10 µM CLV3p12 and CLV3p12$_{Thr6}$ peptides, respectively, were performed as previously described (Song et al., 2012). For competition assays, L*er* wildtype seedlings were treated with different concentrations of CLV3p12$_{Thr6}$ combined with 10 µM CLV3p in liquid 1/2 MS media. Media with peptides were refreshed every day. After a 9-d treatment, shoot apices were excised under a dissection microscope, cleared, and observed as previously described (Sabatini et al., 1999).

GUS Assay

Seedlings and inflorescences of L*er* wildtype*, clv3-2* and *CLV3*$_{Thr6}$ transgenic plants carrying *pCLV3::GUS* (Lenhard et al., 2002) were examined for *GUS* expression as previously described (Fiers et al., 2004). Roots of Col-0 wildtype and *CLE22*$_{Thr6}$ transgenic plants carrying *DR5::GUS* were examined for *GUS* expression as previously described (Ulmasov et al., 1997). After the dehydration with 70%, 85%, 90%, and 100% ethanol, seedlings were cleared, and observed under a DIC microscope (Sabatini et al., 1999). Inflorescences were observed under a dissection microscope directly following dehydration.

Histological Analyses

Siliques of *CLV3*$_{Thr6}$ transgenic plants were fixed in a modified FAA solution (Liu et al., 1993) for 12 h and embedded in LR White (The London Resin

Company Ltd, England) as described in the manufacturer's manual. Embedded siliques were sectioned at 2 µm thickness using a microtome (Leica EM UC7, Germany), and stained with 0.1% toluidine blue.

Real-time quantitative PCR

An RNA isolation kit (Tiangen, Beijing) was used to extract total RNA from shoot apices excised from seedlings of L*er* wildtype and 30 to 40 *CLV3*$_{Thr6}$transgenicT2 plants. Reverse transcription was performed using a FastQuant RT Kit (Tiangen, Beijing). Real-time quantitative PCR was performed in a Rotor-Gene 3000 Thermocycler (Corbett Research, Shanghai) with a SYBR Premix ExTaq II kit (Takara, Beijing). The relative expression levels were normalized against *EIF4A* through the use of a modified $2^{-\Delta\Delta C}{}_{T}$ method (Livak and Schmittgen, 2001). The primers used are listed in Table S1.

Supplemental Data

Fig. S1. Real-time quantitative PCR analyses of *CLV3* and *CLV3*$_{Thr6}$ transgene expression in the wildtype and *CLV3*$_{Thr6}$ transgenic plants

Fig. S2. *In vitro* competition assay

Fig. S3. Alignments of the conserved core CLE motifs in CLE family members

Fig. S4. Alignments of the conserved motifs in AtPEPs and EPFs family members

Table S1. List of primers used

ACKNOWLEDGMENTS

We thank Da-Li Yu and Chen Li for assistance and John Hugh Snyder for critical reading of the manuscript.

LITERATURE CITED

Boller T, Felix G (2009) A renaissance of elicitors: perception of microbe-associated molecular patterns and danger signals by pattern-recognition receptors. Annu Rev Plant Biol **60:** 379-406

Chu H, Qian Q, Liang W, Yin C, Tan H, Yao X, Yuan Z, Yang J, Huang H, Luo D, Ma H, Zhang D (2006) The *FLORAL ORGAN NUMBER4* gene encoding a putative ortholog of Arabidopsis CLAVATA3 regulates apical meristem size in rice. Plant Physiol **142:** 1039-1052

Clark SE, Running MP, Meyerowitz EM (1993) CLAVATA1, a regulator of meristem and flower development in Arabidopsis. Development **119:** 397-418

Clough SJ, Bent AF (1998) Floral dip: a simplified method for *Agrobacterium tumefaciens*-mediated transformation of *Arabidopsis thaliana*. Plant J **16:** 735-743

Cock JM, McCormick S (2001) A large family of genes that share homology with *CLAVATA3*. Plant Physiol **126:** 939-942

De Smet I, Voß U, Jürgens G, Beeckman T (2009) Receptor-like kinases shape the plant. Nat Cell Biol **11:** 1166-1173

Edlund T, Jessell TM (1999) Progression from extrinsic to intrinsic signaling in cell fate specification: a view from the nervous system. Cell **96:** 211-224

Etchells JP, Turner SR (2010) The PXY-CLE41 receptor ligand pair defines a multifunctional pathway that controls the rate and orientation of vascular cell division. Development **137:** 767-774

Evavold BD, Sloan-Lancaster J, Allen PM (1993) Tickling the TCR: selective T-cell functions stimulated by altered peptide ligands. Immunol Today **14:** 602-609

Feld S, Hirschberg R (1996) Growth hormone, the insulin-like growth factor system, and the kidney. Endocr Rev **17:** 423-480

Fiers M, Golemiec E, Xu J, van der Geest L, Heidstra R, Stiekema W, Liu CM (2005) The 14-AA CLV3, CLE19, and CLE40 peptides trigger consumption of the root meristem in Arabidopsis through a CLAVATA2-dependent pathway. Plant Cell **17:** 2542-2553

Fiers M, Hause G, Boutilier K, Casamitjana-Martinez E, Weijers D, Offringa D, van der Geest L, van Lookeren Campagne M, Liu CM (2004) Mis-expression of the *CLV3/ESR*-like gene *CLE19* in Arabidopsis leads to a consumption of root meristem. Gene **327:** 37-49

Fiume E, Fletcher JC (2012) Regulation of Arabidopsis embryo and endosperm development by the polypeptide signaling molecule CLE8. Plant Cell **24:** 1000-1012

Fletcher JC, Brand U, Running MP, Simon R, Meyerowitz EM (1999) Signaling of cell fate decisions by CLAVATA3 in Arabidopsis shoot meristems. Science **283:** 1911-1914

Hara K, Kajita R, Torii KU, Bergmann DC, Kakimoto T (2007) The secretory peptide gene *EPF1* enforces the stomatal one-cell-spacing rule. Genes Dev **21:** 1720-1725

Hobe M, Muller R, Grunewald M, Brand U, Simon R (2003) Loss of CLE40, a protein functionally equivalent to the stem cell restricting signal CLV3, enhances root waving in Arabidopsis. Dev Genes Evol **213:** 371-381

Huffaker A, Ryan CA (2007) Endogenous peptide defense signals in Arabidopsis differentially amplify signaling for the innate immune response. Proc Natl Acad Sci USA **104:** 10732-10736

Jeong S, Trotochaud AE, Clark SE (1999) The Arabidopsis *CLAVATA2* gene encodes a receptor-like protein required for the stability of the CLAVATA1 receptor-like kinase. Plant Cell **11:** 1925-1933

Jun JH, Fiume E, Roeder AHK, Meng L, Sharma VK, Osmont KS, Baker C, Ha CM, Meyerowitz EM, Feldman LJ, Fletcher JC (2010) Comprehensive analysis of *CLE* polypeptide signaling gene expression and overexpression activity in Arabidopsis. Plant Physiol **154:** 1721-1736

Karimi M, Inzè D, Depicker A (2002) Gateway vectors for *Agrobacterium*-mediated plant transformation. Trends Plant Sci**7:** 193-195

Katsir L, Davies KA, Bergmann DC, Laux T (2011) Peptide signaling in plant development. Curr Biol **21:** 356-364

Kinoshita A, Nakamura Y, Sasaki E, Kyozuka J, Fukuda H, Sawa S (2007) Gain-of-function phenotypes of chemically synthetic CLAVATA3/ESR-related (CLE) peptides in *Arabidopsis thaliana* and *Oryza sativa*. Plant Cell Physiol **48:** 1821-1825

Kinoshita A, Betsuyaku S, Osakabe Y, Mizuno S, Nagawa S, Stahl Y, Simon R, Yamaguchi-Shinozaki K, Fukuda H, Sawa S (2010) RPK2 is an essential receptor-like kinase that transmits the CLV3 signal in Arabidopsis. Development **137:** 3911-3920

Kondo T, Sawa S, Kinoshita A, Mizuno S, Kakimoto T, Fukuda H, Sakagami Y (2006) Plant peptide encoded by *CLV3* identified by in situ MALDI-TOF MS analysis. Science **313:** 845-848

Lease KA, Walker JC (2006) The Arabidopsis unannotated secreted peptide database, a resource for plant peptidomics. Plant Physiol **142:** 831-838

Lenhard M, Jürgens G, Laux T (2002) The *WUSCHEL* and *SHOOTMERISTEMLESS* genes fulfill complementary roles in Arabidopsis shoot meristem regulation. Development **129:** 3195-206

Liu C, Xu Z, Chua NH (1993) Auxin polar transport is essential for the establishment of bilateral symmetry during early plant embryogenesis. Plant Cell **5:** 621-630.

Livak KJ, Schmittgen TD (2001) Analysis of relative gene expression data using real-time quantitative PCR and the $2^{-\Delta\Delta C}{}_T$ method. Methods **25:** 402-408

Matsubayashi Y (2011) Post-translational modifications in secreted peptide hormones in plants. Plant Cell Physiol**52:** 5-13

Miwa H, Betsuyaku S, Iwamoto K, Kinoshita A, Fukuda H, Sawa S (2008) The receptor-like kinase SOL2 mediates CLE signaling in Arabidopsis. Plant Cell Physiol **49:** 1752-1757

Müller R, Bleckmann A, Simon R (2008) The receptor kinase CORYNE of Arabidopsis transmits the stem cell-limiting signal CLAVATA3 independently of CLAVATA1. Plant Cell **20:** 934-946

Oelkers K, Goffard N, Weiller GF, Gresshoff PM, Mathesius U, Frickey T (2008) Bioinformatic analysis of the CLE signaling peptide family. BMC Plant Biol**8:** 1-15

Ohyama K, Shinohara H, Ogawa-Ohnishi M, Matsubayashi Y (2009) A glycopeptide regulating stem cell fate in *Arabidopsis thaliana*. Nat Chem Bio **5:** 578-580

Pearce G, Ryan CA (2003) Systemic signaling in tomato plants for defense against herbivores. J Biol Chem **278:** 30044-30050

Sabatini S, Beis D, Wolkenfelt H, Murfett J, Guilfoyle T, Malamy J, Benfey PN, Leyser O, Bechtold N, Weisbeek P, Scheres B (1999) An auxin-dependent distal organizer of pattern and polarity in the Arabidopsis root. Cell **99:** 463-472

Shinohara H. Matsubayashi Y (2012) Chemical synthesis of Arabidopsis CLV3 glycopeptide reveals the impact of Hyp arabinosylation on peptide conformation and activity. Plant Cell Physiol **doi:** 10.1093/pcp/pcs174

Song XF, Yu DL, Xu TT, Ren SC, Guo P, Liu CM (2012) Contributions of individual amino acid residues to the endogenous CLV3 function in shoot apical meristem maintenance in Arabidopsis. Mol Plant **5:** 515-523

Strabala TJ, O'Donnell PJ, Smit AM, Ampomah-Dwamena C, Martin EJ, Netzler N, Nieuwenhuizen NJ, Quinn BD, Foote HCC, Hudson KR (2006) Gain-of-function phenotypes of many *CLAVATA3/ESR* genes, including four new family members, correlate with tandem variations in the conserved CLAVATA3/ESR domain. Plant Physiol **140:** 1331-1344.

Suzaki T, Ohneda M, Toriba T, Yoshida A, Hirano HY (2009) *FON2 SPARE1* redundantly regulates floral meristem maintenance with *FLORAL ORGAN NUMBER2* in rice. PLoS Genet **5:** e1000693

Suzaki T, Yoshida A, Hirano HY (2008) Functional diversification of CLAVATA3-related CLE proteins in meristem maintenance in rice. Plant Cell **20:** 2049-2058

Ulmasov T, Murfett J, Hagen G, Guilfoyle TJ (1997) Aux/IAA proteins repress expression of reporter genes containing natural and highly active synthetic auxin response elements. Plant Cell **9:** 1963-1971.

Yang H, Matsubayashi Y, Nakamura K, Sakagami Y (2001) Diversity of Arabidopsis genes encoding precursors for phytosulfokine, a peptide growth factor. Plant Physiol **127:** 842–851

Zhu Y, Wang Y, Li R, Song X, Wang Q, Huang S, Jin JB, Liu CM, Lin J (2010) Analysis of interactions among the CLAVATA3 receptors reveals a direct interaction between CLAVATA2 and CORYNE in Arabidopsis. Plant J **61:** 223-233

FIGURE LEGENDS

Figure 1. AA-substituted *CLV3* constructs and transgenic analyses in the wildtype. A, Constructs made for two-dimensional substitutions of *CLV3.* A full-length *CLV3* genomic sequence (*CLV3F*) including endogenous regulatory elements was used as the template for first dimensional Ala substitutions in the 12-AA peptide-coding region of CLV3 (named $CLV3_{Ala1\text{-}12}$) and second dimensional substitutions of the Gly residue at the position 6 with all other 18 possible proteinacious AAs. B, Effects of 12 Ala-substituted CLV3 in generating dominant-negative *clv3*-like multi-carpel phenotypes in the wildtype. For each Ala-substituted CLV3, at least 30 transformants were obtained. The wildtype (L*er*), *clv3-2* and *CLV3F* transgenic plants were used as controls. C and D, Wildtype plant (C) with two-carpel siliques (insert in C) and the $CLV3_{Ala6}$ transgenic plant (D) with multi-carpel siliques (insert in D). Bars = 10 mm for C and D; Bars = 0.7 mm for the inset of C and D. E and F, Inflorescences of the wildtype (E) and the BC1 plant of the $CLV3_{Ala6}$ transgenic line (F). Bars = 2 mm.

Figure 2. Antagonistic effects and complementation efficiencies of second dimensional AA-substituted constructs. A, Effects of 18 second dimensional AA-substituted CLV3 in generating the multi-carpel *clv3*-like phenotype in the wildtype. B, Effects of second dimensional AA-substituted CLV3 in complementing *clv3-2* mutants. For each AA-substituted CLV3, at least 30 independent transformants were obtained. The *CLV3F* was used as a control.

Figure 3. Effects of $CLV3_{Thr6}$ in generating the *clv3*-like phenotype. A, Among 43 individual plants transformed with $CLV3_{Thr6}$ examined, 30 showed a multi-carpel *clv3*-like phenotype. Note that wildtype Arabidopsis has two carpels in siliques, the antagonistic effect was observed in transgenic lines with more than 2 carpels. The diamond indicates the average carpel number, while the upper and lower bars represent the most and least carpel numbers, respectively. B, Transverse sections through siliques from $CLV3_{Thr6}$ transgenic plants with three (middle) and seven (right) carpels, as compared to the wildtype (left) with two carpels. The red curves indicate the carpels. Bars = 200 µm. C, Inflorescences of wildtype, $CLV3_{Thr6}$ transgenic, and *clv3-2* plants.

Compared to the wildtype (left), inflorescences in *CLV3*$_{Thr6}$ transgenic plants (middle) had supernumerary flowers, as observed in *clv3-2* mutants (right). Bars = 3 mm. D, A DIC image showing the enlarged SAM in the *CLV3*$_{Thr6}$ transgenic plant (middle), as compared to those from the wildtype (left) and *clv3-2* (right). Arrowheads indicate the margins of SAMs. Bars = 50 μm.

Figure 4. *GUS* expression in inflorescences and SAMs of the wildtype, *CLV3*$_{Thr6}$ transgenic, and *clv3-2* plants carrying *pCLV3::GUS.* A, *GUS* expression in inflorescences. Compared with the wildtype (left), extended *GUS* expression were observed in flower buds of *CLV3*$_{Thr6}$ transgenic plants (middle), as in *clv3-2* (right). Pictures were taken under a dissection microscope. Bars = 3 mm. B, *GUS* expression in SAMs. Compared to the wildtype (left), the *GUS* expression domain was significantly enlarged in the SAM of *CLV3*$_{Thr6}$ transgenic plants (middle), similar to *clv3-2* (right). Pictures were taken under a DIC microscope after clearing. Bars = 150 μm.

Figure 5. Enlarged SAMs observed in wildtype seedlings treated with synthetic CLV3p12$_{Thr6}$ peptides *in vitro.* A, Boxplots of the areas of SAMs in wildtype seedlings treated with CLV3p12, or CLV3p12$_{Thr6}$ peptides, in comparison to those in the wildtype and *clv3-2* seedlings. Areas of SAMs were measured with ImageJ software after pictures of median sections were taken under a DIC microscope. B, DIC images of shoot apices from wildtype seedlings treated with CLV3p12 (top left) or CLV3p12$_{Thr6}$ (top right) for 9 days, compared with untreated ones in the wildtype (bottom left) and *clv3-2* (bottom right). Arrowheads indicate margins of SAMs. Bars = 50 μm.

Figure 6. The embryo-lethal phenotypes in *CLE8*$_{Thr6}$ transgenic plants. A and B, An opened silique of *CLE8*$_{Thr6}$ transgenic plant (A), showing green wildtype ovules and transparent aborted ovules (indicated by arrowheads), as compared to the wildtype silique (B) at the same stage. Bars = 1 mm. C-F, In *CLE8*$_{Thr6}$ transgenic plants, both wildtype (C) and abnormal embryos (D, E and F) were observed in siliques 5 days after pollination. Bars = 50 μm. (G-I) A wildtype cotyledonary embryo (G) and embryos with abnormal cell division pattern (H and I) in the same silique from a *CLE8*$_{Thr6}$ transgenic plant. Bars = 50 μm.

Figure 7. *CLE22*$_{Thr6}$ transgenic plants exhibited a short-root phenotype. A, Progeny of one *CLE22*$_{Thr6}$ transgenic plant, showing different degrees of the short-root phenotype. Bar = 5 mm. B, A seedling of a *CLE22*$_{Thr6}$ transgenic plant, showing termination of the primary root (arrowhead). Bar = 1 mm. C and D, Compared with the root meristems in Col-0 wildtype (C), *CLE22*$_{Thr6}$ transgenic plants (D) showed the aberrant root meristem (arrowhead). Bar = 50 μm. E and F, *DR5::GUS* expression in root meristems in Col-0 wildtype (E) and *CLE22*$_{Thr6}$ transgenic (F) plants, showing the absence of *GUS* expression in the primary root meristem in the transgenic plant (arrowhead). Bar = 50 μm. 5-d old seedlings were used for phenotypic observation and expression analyses.

Figure 8. Schematic model of the antagonistic peptide technology. A, Endogenous CLE peptides (green) bind to its receptors, leading to downstream signal transduction. B, Peptides with the Gly to Thr substitution (red) bind more tightly and competitively to the receptors, but fail to trigger downstream signal transduction.

Figure S1. Real-time quantitative PCR analyses of endogenous *CLV3* and *CLV3$_{Thr6}$* transgene expression in the wildtype and *CLV3$_{Thr6}$* transgenic plants. A, Real-time quantitative PCR results showed that there was no significant difference in the expression level of *CLV3* in L*er* wildtype and *CLV3$_{Thr6}$* transgenic plants (p=0.182). The expression of *CLV3$_{Thr6}$* transgene was higher than endogenous *CLV3* in *CLV3$_{Thr6}$* transgenic plants. B and C, Melting curve analysis of *CLV3* amplification in L*er* wildtype (B) and *CLV3$_{Thr6}$* transgenic plants (C). D and E, Melting curve analysis of *CLV3$_{Thr6}$* amplification in L*er* wildtype (D) and *CLV3$_{Thr6}$* transgenic plants (E). Note that there is no specific amplification of *CLV3$_{Thr6}$* in L*er* wildtype.

Figure S2. *In vitro* competition assay. L*er* wildtype seedlings were treated with 10 µM CLV3p12 + 1µM CLV3p12$_{Thr6}$, 10 µM CLV3p12 + 5µM CLV3p12$_{Thr6}$ and 10 µM CLV3p12 + 10 µM CLV3p12$_{Thr6}$, respectively. The meristem size of 500 um^2 was used to assign meristems with a significant reduction after peptide treatments. The percentage of SAMs larger than 500 µm^2 was increased significantly as compared with those treated only with 10 µM CLV3p12.

Figure S3. Alignments of the core CLE motifs in CLE family members. The blue box indicates the Gly residue (90.4% identity among 198 CLEs) in the core CLE motif of CLE family members identified in *Chlamydomonas*, moss, angiosperm and nematode. OS: *Oryza sativa*; AT: *Arabidopsis thaliana*; GM: *Glycine max*; ZM: *Zea mays*; PV: *Phaseolus vulagaris*; MT: *Medicago truncatula*; PT: *Populus trichocarpa*; BN: *Brassica napus*; LE: *Lycopersicum esculentum*; LC: *Phaseolus coccineus*; Hg: *Heterodera glycines*; NT: *Nicotianatabacum*; ST: *Solanum tuberosum*; TA: *Tritium aestivum*; PC: *Phaseoluscoccineus*; GH: *Gossypium hirsutum*; PP: *Physcomitrella patens*; CR: *Chlamydomonas reinhardtii*; Ze: *Zinnia elegans*.

Figure S4. Alignments of the conserved motifs in AtPEPs and EPFs family members. A, The red box indicates the glycine residue in AtPEPs family members. B, The red boxes indicate glycine residues in EPFs family members. At: *Arabidopsis thaliana*; Os: *Oryza sativa*; Pp: *Physcomitrella patens*; Sm: *Selaginella moellendorffii.*

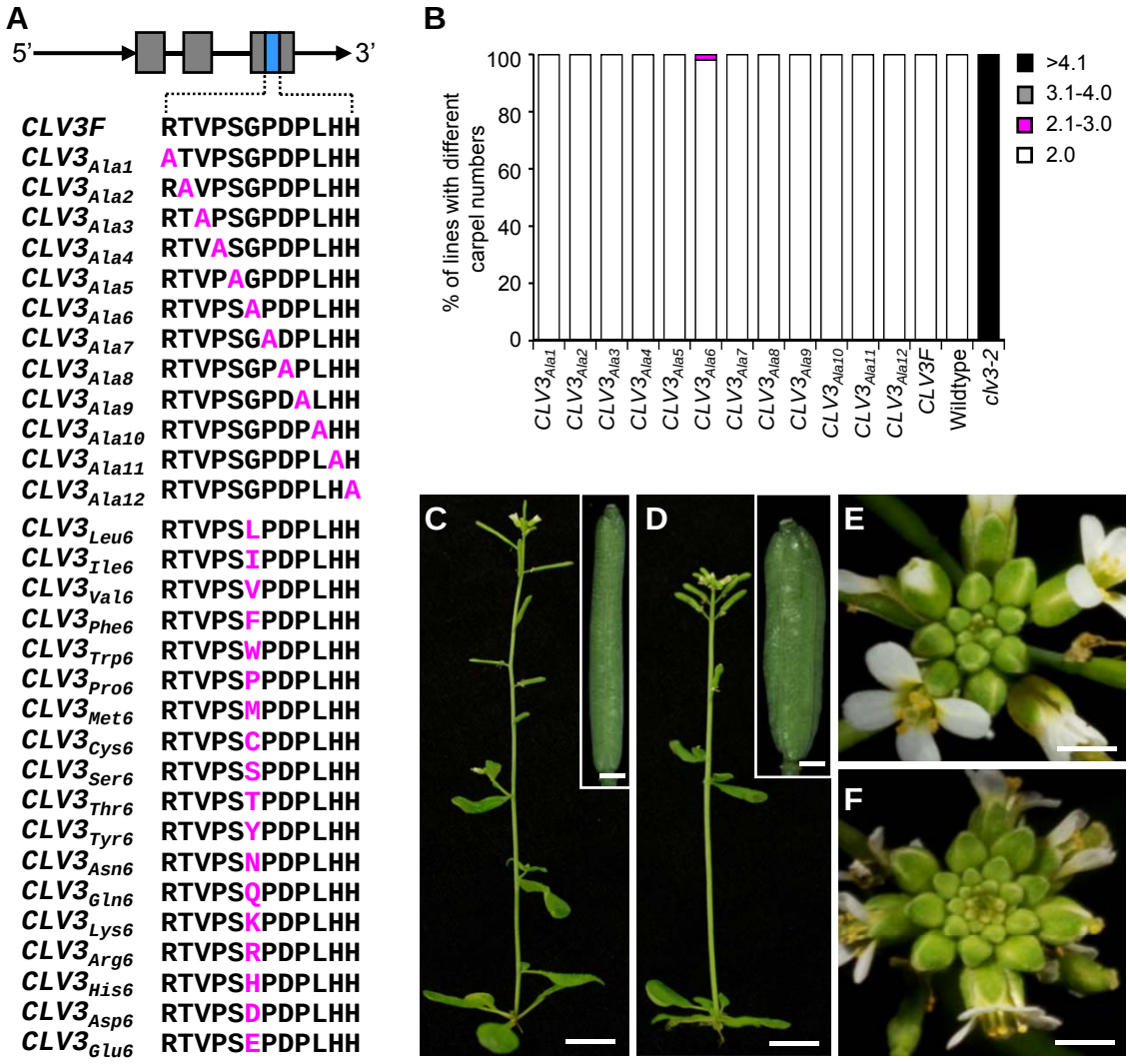

Figure 1. AA-substituted *CLV3* constructs and transgenic analyses in the wildtype. A, Constructs made for two-dimensional substitutions of *CLV3.* A full-length *CLV3* genomic sequence (*CLV3F*) including endogenous regulatory elements was used as the template for first dimensional Ala substitutions in the 12-AA peptide-coding region of CLV3 (named $CLV3_{Ala1\text{-}12}$) and second dimensional substitutions of the Gly residue at the position 6 with all other 18 possible proteinacious AAs. B, Effects of 12 Ala-substituted CLV3 in generating dominant-negative *clv3*-like multi-carpel phenotypes in the wildtype. For each Ala-substituted CLV3, at least 30 transformants were obtained. The wildtype (L*er*), *clv3-2* and *CLV3F* transgenic plants were used as controls. C and D, Wildtype plant (C) with two-carpel siliques (insert in C) and the $CLV3_{Ala6}$ transgenic plant (D) with multi-carpel siliques (insert in D). Bars = 10 mm for C and D; Bars = 0.7 mm for the inset of C and D. E and F, Inflorescences of the wildtype (E) and the BC1 plant of the $CLV3_{Ala6}$ transgenic line (F). Bars = 2 mm.

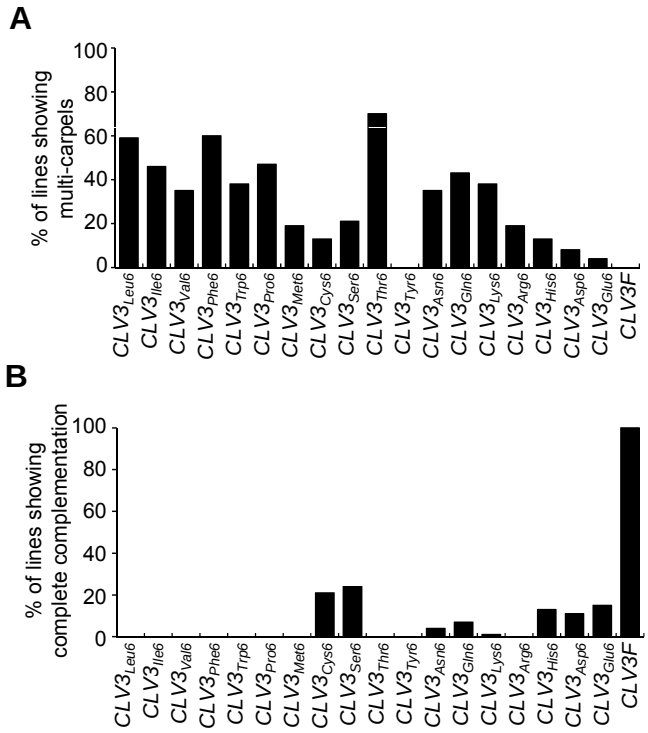

Figure 2. Antagonistic effects and complementation efficiencies of second dimensional AA-substituted constructs. A, Effects of 18 second dimensional AA-substituted CLV3 in generating the multi-carpel *clv3*-like phenotype in the wildtype. B, Effects of second dimensional AA-substituted CLV3 in complementing *clv3-2* mutants. For each AA-substituted CLV3, at least 30 independent transformants were obtained. The *CLV3F* was used as a control.

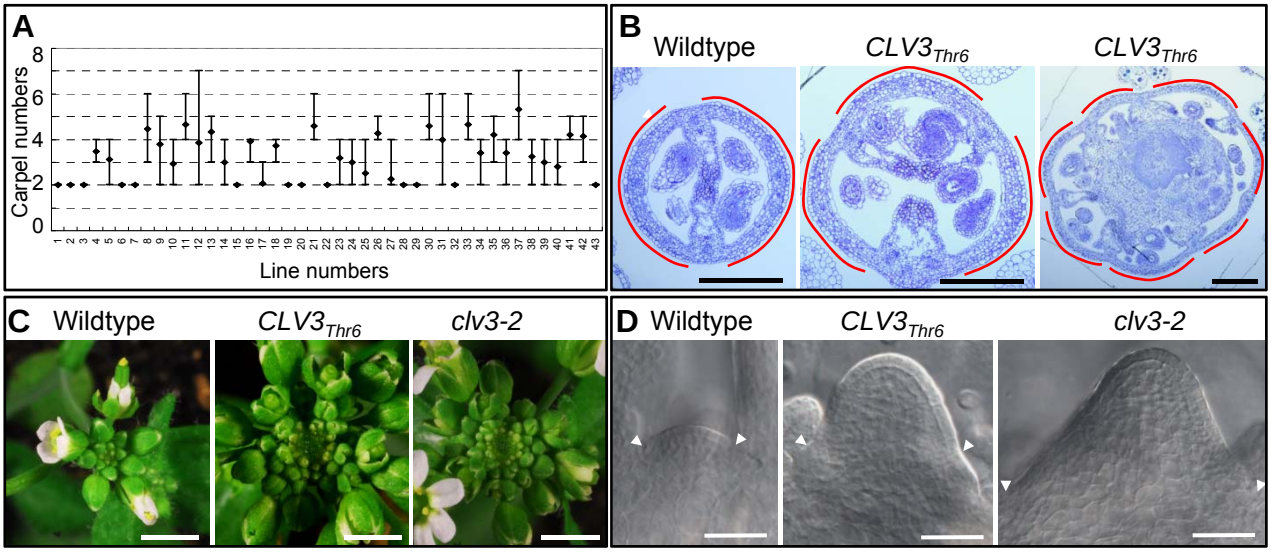

Figure 3. Effects of *CLV3*$_{Thr6}$ in generating the *clv3*-like phenotype. A, Among 43 individual plants transformed with *CLV3*$_{Thr6}$ examined, 30 showed a multi-carpel *clv3*-like phenotype. Note that wildtype Arabidopsis has two carpels in siliques, the antagonistic effect was observed in transgenic lines with more than 2 carpels. The diamond indicates the average carpel number, while the upper and lower bars represent the most and least carpel numbers, respectively. B, Transverse sections through siliques from *CLV3*$_{Thr6}$ transgenic plants with three (middle) and seven (right) carpels, as compared to the wildtype (left) with two carpels. The red curves indicate the carpels. Bars = 200 μm. C, Inflorescences of wildtype, *CLV3*$_{Thr6}$ transgenic, and *clv3-2* plants. Compared to the wildtype (left), inflorescences in *CLV3*$_{Thr6}$ transgenic plants (middle) had supernumerary flowers, as observed in *clv3-2* mutants (right). Bars = 3 mm. D, A DIC image showing the enlarged SAM in the *CLV3*$_{Thr6}$ transgenic plant (middle), as compared to those from the wildtype (left) and *clv3-2* (right). Arrowheads indicate the margins of SAMs. Bars = 50 μm.

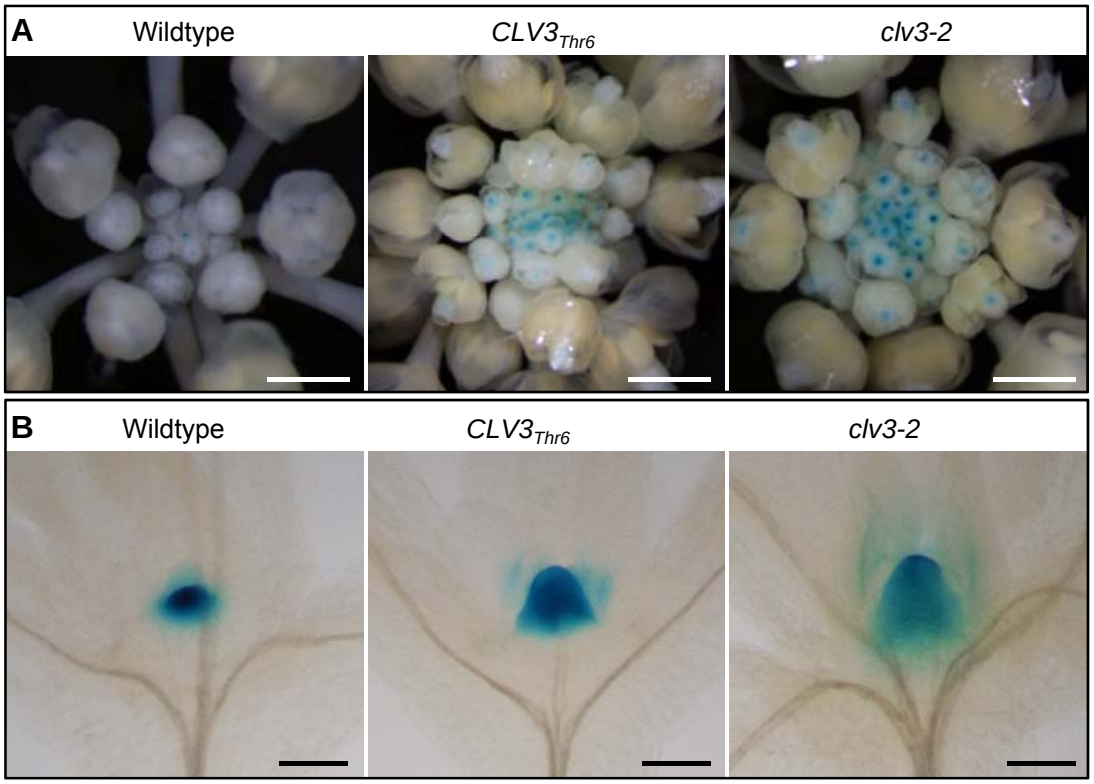

Figure 4. *GUS* expression in inflorescences and SAMs of the wildtype, $CLV3_{Thr6}$ transgenic, and *clv3-2* plants carrying *pCLV3::GUS.* A, *GUS* expression in inflorescences. Compared with the wildtype (left), extended *GUS* expression were observed in flower buds of $CLV3_{Thr6}$ transgenic plants (middle), as in *clv3-2* (right). Pictures were taken under a dissection microscope. Bars = 3 mm. B, *GUS* expression in SAMs. Compared to the wildtype (left), the *GUS* expression domain was significantly enlarged in the SAM of $CLV3_{Thr6}$ transgenic plants (middle), similar to *clv3-2* (right). Pictures were taken under a DIC microscope after clearing. Bars = 150 μm.

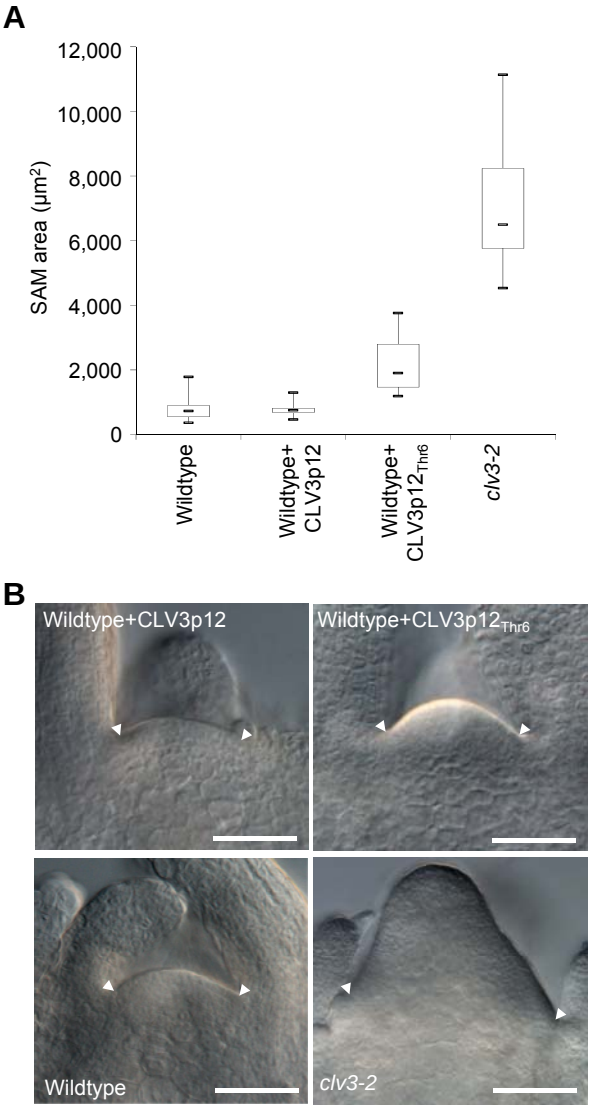

Figure 5. Enlarged SAMs observed in wildtype seedlings treated with synthetic CLV3p12$_{Thr6}$ peptides *in vitro.* A, Boxplots of the areas of SAMs in wildtype seedlings treated with CLV3p12, or CLV3p12$_{Thr6}$ peptides, in comparison to those in the wildtype and *clv3-2* seedlings. Areas of SAMs were measured with ImageJ software after pictures of median sections were taken under a DIC microscope. B, DIC images of shoot apices from wildtype seedlings treated with CLV3p12 (top left) or CLV3p12$_{Thr6}$ (top right) for 9 days, compared with untreated ones in the wildtype (bottom left) and *clv3-2* (bottom right). Arrowheads indicate margins of SAMs. Bars = 50 µm.

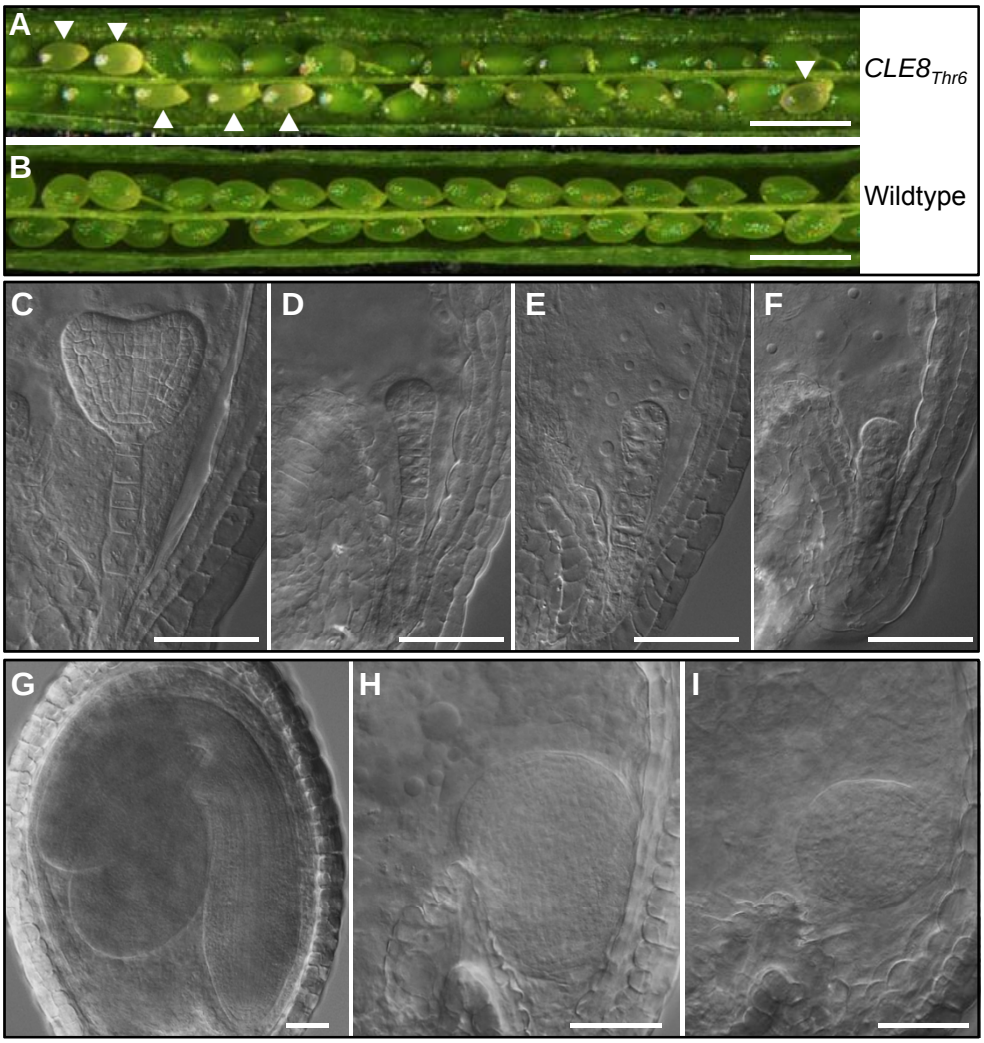

Figure 6. The embryo-lethal phenotypes in *CLE8*$_{Thr6}$ transgenic plants. A and B, An opened silique of *CLE8*$_{Thr6}$ transgenic plant (A), showing green wildtype ovules and transparent aborted ovules (indicated by arrowheads), as compared to the wildtype silique (B) at the same stage. Bars = 1 mm. C-F, In *CLE8*$_{Thr6}$ transgenic plants, both wildtype (C) and abnormal embryos (D, E and F) were observed in siliques 5 days after pollination. Bars = 50 μm. (G-I) A wildtype cotyledonary embryo (G) and embryos with abnormal cell division pattern (H and I) in the same silique from a *CLE8*$_{Thr6}$ transgenic plant. Bars = 50 μm.

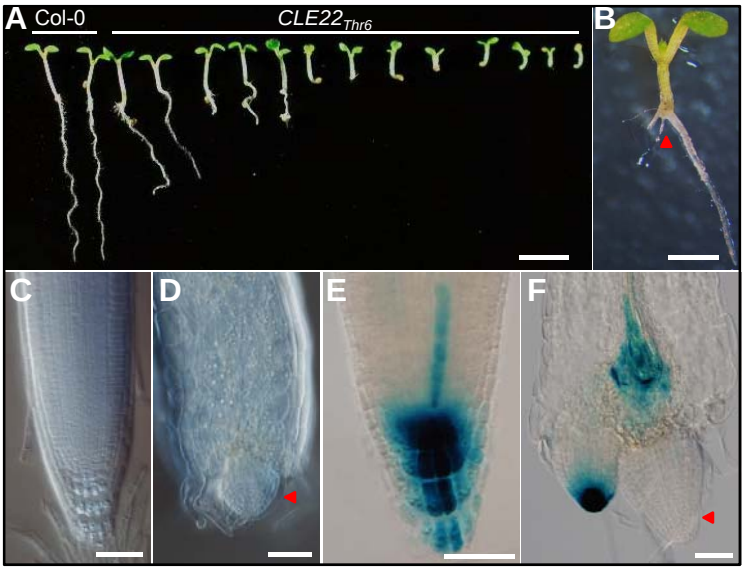

Figure 7. *CLE22*$_{Thr6}$ transgenic plants exhibited a short-root phenotype. A, Progeny of one *CLE22*$_{Thr6}$ transgenic plant, showing different degrees of the short-root phenotype. Bar = 5 mm. B, A seedling of a *CLE22*$_{Thr6}$ transgenic plant, showing termination of the primary root (arrowhead). Bar = 1 mm. C and D, Compared with the root meristems in Col-0 wildtype (C), *CLE22*$_{Thr6}$ transgenic plants (D) showed the aberrant root meristem (arrowhead). Bar = 50 μm. E and F, *DR5::GUS* expression in root meristems in Col-0 wildtype (E) and *CLE22*$_{Thr6}$ transgenic (F) plants, showing the absence of *GUS* expression in the primary root meristem in the transgenic plant (arrowhead). Bar = 50 μm. 5-d old seedlings were used for phenotypic observation and expression analyses.

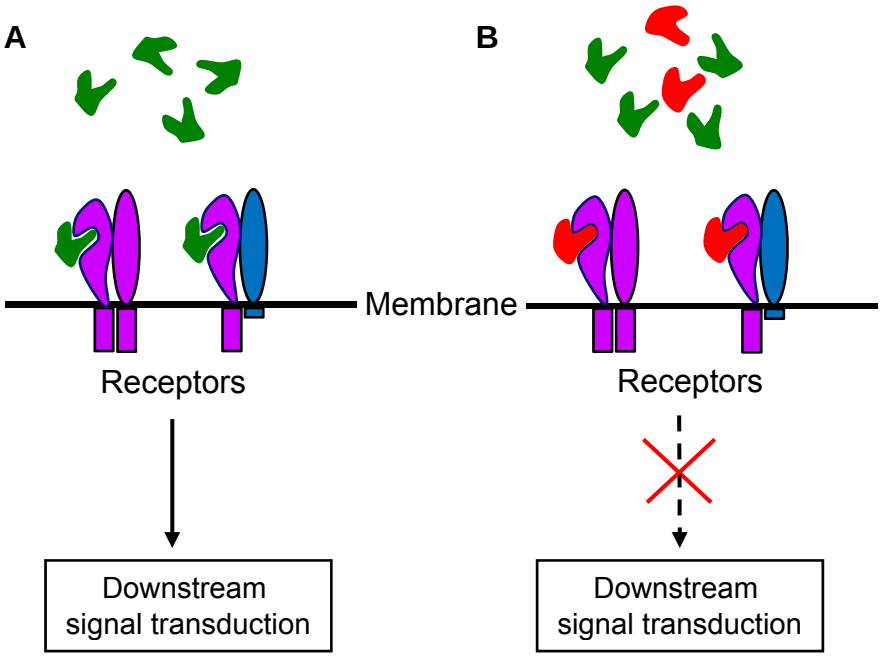

Figure 8. Schematic model of the antagonistic peptide technology. A, Endogenous CLE peptides (green) bind to its receptors, leading to downstream signal transduction. B, Peptides with the Gly to Thr substitution (red) bind more tightly and competitively to the receptors, but fail to trigger downstream signal transduction.